*Nuclear Mathematical and Computational Sciences: A Century in Review, A Century Anew*
Gatlinburg, Tennessee, April 6-11, 2003, on CD-ROM, American Nuclear Society, LaGrange Park, IL (2003)

# Implementation of IAEA Photonuclear Data Compilations to the RTS&T General-Purpose Transport Code, Test Calculations of Photoneutrons Emission from Surface of Uranium Sphere Irradiated by 28 MeV Electrons

I.I. Degtyarev
Institute for High Energy Physics
142284 Protvino, Russia
degtyarev@mx.ihep.su

A.I. Blokhin
Institute of Physics and Power Engineering
249020 Obninsk, Russia
blokhin@ippe.obninsk.ru

## ABSTRACT

In this paper reported a present status of the RTS&T photonuclear data-driven model and verification results for the BOFOD photonuclear data files obtained for the uranium isotopes $U^{235}$, $U^{238}$. This result was compared with calculated data obtained by the parametrization-driven model of photonuclear reaction and experimental data of photoneutron yields from surface of uranium sphere irradiated by 28 MeV electrons. Both calculations have been carried out with RTS&T general-purpose code to detailed electron-photon-nucleon transport using the ENDF/B-VI and EPDL evaluated data libraries.

*Key Words*: photonuclear reactions, Monte Carlo simulation

## 1. RTS&T PHOTONUCLEAR REACTION MODELS

Inelastic photonic interactions are simulated within RTS&T [1] code by several energy-dependent models based on the different microscopic and macroscopic approaches: using a set of the semi-empirical parametrizations for inclusive cross sections and multiplicities (mainly for the neutron-emission channels description) [Parametrization-Driven Model (PDM)], a cascade-exciton model of photonuclear reactions [CEM-RTS&T]. Additionally, the Dual-Parton model [DPMJET-II.5] can be used for simulating of high-energy photon induced reactions.

### 1.1. Parametrization-driven Model (PDM) of low- and intermediate-energy photonic interactions

PDM performs a fast inclusive simulation of final-state parameters for secondary particles produced in photonuclear interactions in the energy range from threshold energy of GDR-particle emission to several GeV.

Total cross sections of $(\gamma, in)$-channels in GDR region is calculated from the formula: $\sigma(\gamma, in) = \sigma_{abs} \cdot P(E, i)$, where $\sigma_{abs}$, $P$ are the absorption cross section and probability of $i$-neutrons equilibrium emission given by Jackson's analytical expression [2]:

$$P(E,i) = I(\Delta_i, 2i-3) - I(\Delta_{i+1}, 2i-1),$$

where $I(z,n) = (1/n!)\int_0^z y^n e^{-y} dy$ is incomplete gamma-function, and

$\Delta_k = [(E - \sum_{k=1}^{i} B_k) - E_{thr}^f]/T$. Here, $\overline{E}_x$, $B_k$, $E_{thr}^f$ and $T = [1+(1+4aU)^{1/2}]/2a$ are the average excitation energy, the binding energy of $i-$th neutron, threshold energy of photofission reaction, and nuclear temperature, determined from the back-shifted Fermi gas model [3], respectively. $U = \overline{E}_x - \Delta$, where $\Delta$ is a pairing correction. Level density parameter $a$ is taken from the RIPL-recommended systematics as proposed in [4]. The total photoabsorption cross section is to calculate as a sum of three components: $\sigma_{abs} = \sum_{i=1}^{3} \sigma_i$. Components of i=1 to 3 correspond to the GDR, QD and baryon resonance production processes. The GDR term is given by a Lorentz-shape curves. RIPL-recommended compilations of giant resonance parameters are used. The QD component of total photoabsorption cross section calculated from [4]: $\sigma_{QD} = L\frac{NZ}{A}\sigma_d(E_\gamma) f_{Pauli}(E_\gamma)$, where $L = 6.5$ is the Levinger parameter, $NZ$ is the number of neutron-proton pairs in the nucleus, $\sigma_d$ is the free deuteron photodisintegration $\gamma d \to np$ cross section (mb): $\sigma_d(E_\gamma) = \frac{C(E_\gamma - E_{thr})^{3/2}}{E_\gamma^3}$, where $E_{thr} = 2.226$ MeV is the threshold energy and $C$ is a constant equal 62.4. $f_{Pauli}$ is the Pauli-blocking function:

$$f_{Pauli} = \begin{cases} a_0 + \sum_{i=1}^{4} a_i E_\gamma^i, & 20 \le E_\gamma \le 140 \ MeV \\ \exp(-\frac{D_p}{E_\gamma}), & otherwise \end{cases}.$$

Constant factor $D_p = 73.3$ if $E_\gamma < 20$ MeV and $D_P = 24.2$ for $E_\gamma > 140$ MeV, $a_i$ are the coefficients of polynomial expansion: $a_0 = 8.3714 \cdot 10^{-2}$, $a_1 = -9.8343 \cdot 10^{-3}$, $a_2 = 4.1222 \cdot 10^{-4}$, $a_3 = -3.4762 \cdot 10^{-6}$, $a_4 = 9.3537 \cdot 10^{-9}$.

In the energy range of $\Delta$-resonance [ $P_{33}(1232)$ ] the cross section can be represented by the following Gaussian function:

$$\frac{\sigma_\Delta}{A} = \sigma_0 + \frac{C}{w\sqrt{\pi/2}} \exp[-\frac{2(E_\gamma - E_c)^2}{w^2}],$$

where $\sigma_0$, $C$, $E_c$ and $w$ are the constant parameters obtained by the least squares fitting as listed in Table 1.

**Table I. Numerical values of the parameters for approximation of $\sigma_\Delta$ in the $\Delta$- region.**

| $\sigma_0$ | $C$ | $E_c$ | $w$ |
|---|---|---|---|
| 28.20001± | 92.87255± | 0.34388± | 0.19358± |
| 3.06707 | 2.13427 | 0.0013 | 0.00309 |

In the energy range of the higher baryon resonances $P_{11}(1440)$, $D_{13}(1520)$, $S_{11}(1535)$, $F_{15}(1680)$, shadowing threshold and shadowing regions the total photoabsorption cross section was parametrized in form: $\sigma_\Delta / A = \sigma_0 \exp(\lambda / E_\gamma)$ ($\mu b$) where $\sigma_0 = 90.0457$ and $\lambda = 0.5378$ are the constant parameters. Fig. 1 shows the total photoabsorption cross section parametrization in comparison with Frascati, Bonn and Mainz [6-10] experimental data.

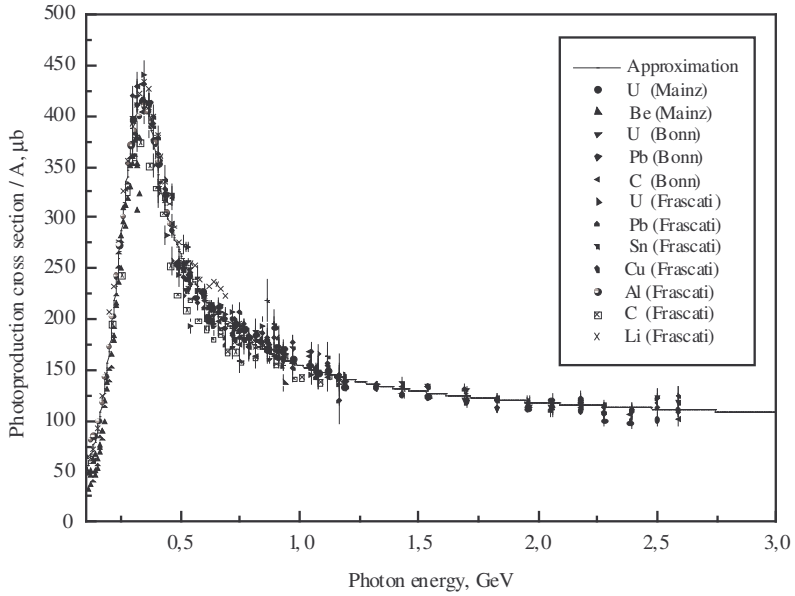


**Figure 1. Total photoabsorption cross section.**

The photofission cross section for the GDR region is parametrized by a sum of two Lorentzian shapes with a parameters derived from analysis of the experimental data using international nuclear data library EXFOR and original publications. Selected evaluated cross sections are also used. Above the GDR energy region (in QD and isobar production regions) it is given as follows,

using the isotope fissility $D_f$: $\sigma_f = D_f \sigma_{abs}$. The total fission probability is expressed by the following relation [11]: $D_f^{QD} = F_2 / F_1$, where

$$F_i = \begin{cases} f_{Pauli}, & i=1 \\ \exp(-\frac{D-\Gamma}{E_\gamma})\{1-\exp(-\frac{D+\Gamma}{E_\gamma})\}, & i=2 \end{cases}.$$

The A-dependence of the fitting parameter $D$ is [12]: $D = 18A^{0.22}/[1+\exp(-0.06A)]$. The energy-depended phenomenological function $\Gamma$ is quadric in $\sqrt{E_\gamma}$:
$\Gamma(E_\gamma) = p_1 + p_2\sqrt{E_\gamma} + p_3 E_\gamma$, where

$$p_i = \begin{cases} p_0 + \frac{C}{w\sqrt{\pi/2}}\exp[-\frac{2(A-A_c)^2}{w^2}], & i=1,3 \\ aA^2 + bA + c, & i=2 \end{cases}$$

In Table 2 the numerical values for $p_i$ parameters are presented. The statistical accuracy is about 10 %.

**Table II. Numerical values of the $p_i$ parameters.**

| i | 1 | 3 | 2 |
|---|---|---|---|
| $p_0$ | 5.96196 | 0.36863 | |
| $A_c$ | 23.39532 | 23.62359 | |
| $w$ | 21.71405 | 21.94853 | |
| $C$ | 4599.96159 | 76.18157 | |
| $a$ | | | 0.0694 |
| $b$ | | | -32.0536 |
| $c$ | | | 3658.581 |

Fig. 2 plots the experimental data of photofission probability for $Bi^{209}$ at different photon energies from 29 to 280 MeV compared to the parametrization.

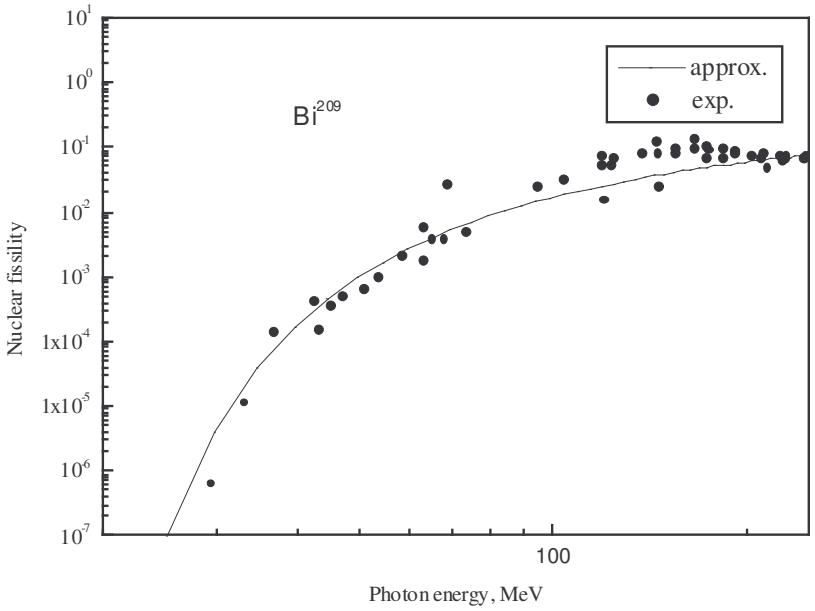


**Figure 2. Nuclear fissility of $Bi^{209}$ as a function of initial photon energy.**

Up to the pion production threshold the nucleon emission cross section

$$(\frac{d^2\sigma}{dEd\Omega})_{QD} = (1-f_{MSD})\frac{1}{4\pi}(\frac{d\sigma}{dE})_{eq} + f_{MSD}\,g(\theta)(\frac{d\sigma}{dE})_{pe},$$

where $f_{MSD}$ is the fraction of the cross section connected with pre-equilibrium processes, $g(\theta)$ is the quasideutron angular distribution is given by:

$$g(\theta) = \frac{1}{4\pi}\cdot\frac{2a}{e^a - e^{-a}}e^{a\cos\theta},$$

where $a$ is the modified [13] parameter of the Kalbach's (1988) systematic for continuum angular distribution:

$$a = a_{Kalbach}\sqrt{\frac{E_\gamma}{2m}}\{\min[4, \max(1, \frac{9.3}{E_{cm}})]\}.$$

Here, $m$ is the neutron mass in MeV units. The angle-integrated spectrum is parametrized using the gamma-distribution [14]:

$$\frac{d\sigma}{d\varepsilon} = (\frac{\varepsilon}{T})^\alpha \frac{\exp(-\varepsilon/T)}{T^{\nu+1}\cdot\Gamma(1+\alpha)},$$

where $\varepsilon = E - VZ_j$, and $j$, $Z_j$, $T$, $V$ are the index and charge of outgoing particle, nuclear temperature and the Coulomb potential on the surface of excited nucleus. The shape parameter of the distribution $\alpha = 0.5$ and $\nu$ is a parameter equal 5 to describe of pre-equilibrium emission spectrum. $\nu = 4$ connected with equilibrium particle production.

Above the pion photoproduction threshold the double differential cross section of particle emission was determined in a form of summation of two components correspond to the QD and pion production ( $\gamma N \to \pi N$, $\gamma N \to \Delta \to i\pi N$ ) mechanisms:

$$\frac{d^2\sigma}{dEd\Omega} = (\frac{d^2\sigma}{dEd\Omega})_{QD} + \sum_i (\frac{d^2\sigma}{dEd\Omega})_{i\pi N} .$$

$$(\frac{d^2\sigma}{dEd\Omega})_{i\pi N} = R(\frac{d^2\sigma}{dEd\Omega})^{\gamma N}_{i\pi N},$$

where $(\frac{d^2\sigma}{dEd\Omega})^{\gamma N}_{i\pi N}$ is the double differential cross section of particle production in the interaction of photon with free nucleon. The INC model [15] predicts a power law for the A-dependence of the differential cross section of nucleon and pion emission: $R \approx A^{\alpha}$, where

$$\alpha = \begin{cases} 0.65, & \pi \\ 1.15, & N \end{cases}.$$

Angular distribution of pions produced in the one-pion channels is expressed as polynomial expansion of type:

$$\frac{d\sigma}{d\Omega} = \frac{1}{(1 - \beta\cos\theta)} \sum_{i=0}^{n} a_i (\cos\theta)^i ,$$

where $\beta$ and $\theta$ are the velocity and scattering angle of the pion in c.m. system. The energy-depended numerical values of the coefficients $a_i$ are given in [16]. For channels, corresponding to multiple pion production, the energy-integrated cross section (c.m.s.) is parametrized in the analytic forms proposed in Ref. [17]:

$$\frac{d\sigma}{d\Omega} = \begin{cases} A + B\cos\theta + C\cos^2\theta + D\cos^3\theta, & E_\gamma \le 1.7\ GeV \\ e^{\alpha+\beta\cos\theta} + 0.43 - 0.12\,W, & E_\gamma > 1.7\ GeV \end{cases}$$

With $W$ is the invariant mass. The coefficients of the expansions are reported in Tables 3,4.

**Table III.** $d\sigma / d\Omega$ **coefficients for the** $\gamma N \to \Delta N \quad (E_\gamma \le 1.7\ GeV)$.

| | W (GeV) | | | |
|---|---|---|---|---|
| | 1.71 | 1.82 | 1.92 | 2.02 |
| A | 1.77 | 0.17 | 0.89 | -0.84 |
| B | 3.09 | 0.84 | -2.01 | 11.7 |
| C | 2.81 | 5.22 | -7.33 | -36.8 |
| D | 0.25 | 5.44 | 22.9 | 38.5 |

**Table IV.** $d\sigma / d\Omega$ **expansion coefficients for the** $\gamma N \to \Delta N \quad (E_\gamma > 1.7\ GeV)$.

| | W (GeV) | | | |
|---|---|---|---|---|
| | 2.02 | 2.22 | 2.55 | 3.05 |
| $\alpha$ | -2.78 | -6.25 | -13.7 | -20.51 |
| $\beta$ | 5.31 | 8.89 | 16.40 | 22.85 |

For two-body final state the emission angle of ligher particle samplied according to the energy-differential cross section and from energy and momentum conservation. For the "quasi-two-body" interactions additionally a value of the invariant mass is sampled from a Breit Wigner distribution and the kinematics is calculated according to the model of Barashenkov et al. [18]. Finally, a decay parameters of the unstable particle is generated and all outgoing characteristics are transformed to laboratory frame.

Average total multiplicity of photoneutron at energies above the pion production threshold can be estimated as follows [19]:

$$\bar{\nu} = \bar{\nu}_{eq} + \bar{\nu}_{pe} + \bar{\nu}_{c},$$

where $\bar{\nu}_{eq}$, $\bar{\nu}_{pe}$ and $\bar{\nu}_{c}$ the average neutron multiplicities of the equilibrium, pre-equilibrium and cascade fractions of the reaction, respectively. As proposed by Lepretre at al [20]

$$\overline{E}_x = \frac{1}{2}\overline{B} + \overline{\nu}_{eq}\overline{B}',$$

where $\overline{B}' = T_n + B_n$ is the average energy removed by an slow neutron (kinetic plus binding energies), $\overline{B}$ is the mean binding energy of the residual nucleus in the evaporation chain, $a$ is the level density parameter. Also,

$$\overline{B}'(\overline{E}_x) = \overline{B} + 2\sqrt{\frac{\overline{E}_x}{a}}$$

Thus,

$$\overline{\nu}_{eq}(\overline{E}_x) = \frac{1}{\overline{B}'(\overline{E}_x)}(\overline{E}_x - \frac{1}{2}\overline{B}).$$

Average excitation energy of the residual nucleus $\overline{E}_x$ is determined as:

$$\overline{E}_x = \begin{cases} E_\gamma, & E_\gamma \le 70\ MeV \\ E_\gamma / 2, & 70 < E_\gamma \le 140\ MeV \\ E_\gamma - \overline{E}_T, & E_\gamma > 140\ MeV \end{cases},$$

where $\overline{E}_T = P_{QD} \cdot \overline{E}_f^{QD} + P_\pi \cdot P_{abs} \cdot \overline{E}_f^{\pi} + P_\pi \cdot (1 - P_{abs}) E_\pi$ is the average total energy lost by the nucleus in the fast stages of reaction. Here $\overline{E}_f^{QD}$ and $\overline{E}_f^{\pi}$ are the average total energies (binding plus kinetic) removed by the cascade nucleons and pion reabsorption processes, respectively. Here, $P_{QD} = \frac{\sigma_{abs}^{QD}}{\sigma_{abs}}$, $P_\pi = \frac{\sigma^{i\pi N}}{\sigma_{abs}}$, and $P_{abs} = 1 - e^{-R/\lambda_\pi}$ with $\sigma_{abs} = \sigma_{abs}^{QD} + \sigma_{abs}^{\Delta}$ are the corresponding probabilities of these processes. $\sigma_{abs}^{QD}$, $\sigma_{abs}^{\Delta}$, $\sigma^{i\pi N}$, $R = r_0 A^{1/3}$ $(fm)$ and $\lambda_\pi = \lambda_\pi(T_\pi)$ are the photoabsorption cross section in the QD and $\Delta$ regions, the pion photoproduction cross section, nuclear radius and the pion average free path inside the nucleus. $\sigma_{abs}^{\pi}(T,Z) = aZ \cdot \sigma_{abs}^{\pi d}$, where $\sigma_{abs}^{\pi d} = 4.1\frac{0.14 + \eta^2}{\eta}$ (mb) is a free deuteron absorption cross section, $\eta = p_\pi / m_\pi$, $a \approx 4$. The direct one-pion production cross section on nucleon $\sigma^{\gamma N \to \pi N}$ was calculated in the framework of the approach described in Ref. [21]. The expansion coefficients of the polynomial fit to the integral cross section of multipion (i=2,10) production $\sigma^{\gamma N \to i\pi N}$ between 0-10 GeV is taken from Ref. [15]. Average multiplicities of cascade particles can be estimated as

$$\overline{\nu}_c^{\pi} = \sum_i i\frac{\sigma^{i\pi N}}{\sigma_{abs}};\ \ \overline{\nu}_c^{p/n} = \sum_i \frac{\sigma^{i\pi N}}{\sigma_{abs}}.$$

Outgoing energy of neutrons for $(\gamma, f)$-channel is sampled from the fission spectrum which is taken in form proposed in Ref. [17]:

$$f(E_\gamma) = \frac{1}{2}\exp[-\frac{f_1(E_\gamma)}{C}]\{\exp[f_2(E_\gamma)] - \exp[-f_2(E_\gamma)]\},$$

where $f_1$ and $f_2$ are the functions of incident photon energy and the threshold energy of photofission channel, $C \approx 0.965$ is normalized factor. Average multiplicity of prompt neutrons per photofission is given by the following expression

$$\bar{\nu}_p(\frac{Z^2}{A}, E_\gamma) = \begin{cases} aE_\gamma + b, & E_\gamma \le 20\ MeV \\ \alpha \ln E_\gamma + \beta, & E_\gamma > 20\ MeV \end{cases},$$

where $a$ and $b$ are the functions of fissionability expressed as polynomial expansions:

$$\begin{cases} a = \sum_{i=0}^{3} a_i (\frac{Z^2}{A})^i \\ b = \sum_{i=0}^{3} b_i (\frac{Z^2}{A})^i \end{cases}$$

and $\alpha = 0.559$, $\beta = 2.569$ are the constant factors. Table 5 reports numerical values for the polynomial coefficients $a_i$ and $b_i$. The average number of prompt gamma rays from fission is approximated as [18]:

$$\bar{G} = \frac{E_t(\bar{\nu}_p, Z, A)}{\bar{E}},$$

where $E_t(\bar{\nu}_p) = \varphi(Z,A)\bar{\nu}_p + 4.0$ is the total prompt gamma rays energy, $\varphi$ is an arbitrary function determined by expression: $\varphi(Z,A) = 2.51(\pm 0.01) - 1.13 \cdot 10^{-5}(\pm 7.2 \cdot 10^{-8})Z^2 A^{1/2}$. Here $A$ and $Z$ are the atomic mass and number of the pre-fission nucleus. The average prompt gamma ray energy is $\bar{E} = -1.33(\pm 0.05) + 119.6(\pm 2.5)Z^{1/3}/A.$ The multiplicity distribution of prompt neutrons and gamma rays from fission is described using the negative binomial distribution:

$$\Pi(n) = \binom{\alpha + n - 1}{n} p^\alpha (1-p)^n,$$

with parameters defined as $p = \frac{\alpha}{\alpha + \bar{n}}$ and $\alpha = (D-1)^{-1}$, where $D$ is the relative width is appoximately 1.04.

**Table 5. Numerical values of the $a_i$ and $b_i$ coefficients.**

| $i$ | $a_i$ | $b_i$ |
|---|---|---|
| 0 | 67208.7929 | -75126.4730 |
| 1 | -5535.87748 | 6328.95964 |
| 2 | 151.98430 | -177.60059 |
| 3 | -1.39079 | 1.66016 |

### 1.2. Data-driven model of low-energy photonic interactions

This model is based on direct use of evaluated nuclear data libraries written in the ENDF-6 format to detailed Monte Carlo modelling of the coupled multy-particles transport and discrete reactions of the particles in the energy range from thermal energy up to 150 MeV. All data types provided by ENDF-6 format are takes account due to radiation transport simulation. A continuous–energy cross section data are used. ENDF data pre-processing (linearization, restoration of the resolved resonances, temperature dependent Doppler broaden of the cross sections, checking and correcting of angular distributions and Legendre coefficients for negative values) is produced automatically with the ENDF pre-processing codes LINEAR, RECENT (RECEN-DD for Reich-Moore parameters of several isotopes of JENDL library only), SIGMA1 and LEGEND [24]. ENDF-recommended interpolation schemes are used to minimize the amount of data. For data storage in memory and their further use the dynamically allocated tree of objects is organized.

### 1.3. High-energy photonic interactions

High-energy photonic interactions are simulated within RTS&T code using the DPMJET (two component Dual Parton Model with JETs) [25]. Version II. 5 of event generator is used.

## 2. ELECTROMAGNETIC INTERACTIONS

In current version (RTS&T 2000) of the RTS&T code following photonic processes are simulated: photoelectric effect from $K$, $L_{I-III}$ atomic shells (fluorescence x-ray yield and tracking is simulated too), Rayleigh scattering, Compton scattering, pair production by photons, interactions of photons with nuclei. The EPDL [26] evaluated data of total cross sections for photon-interactions, coherent and incoherent scattering form-factors are used in the photon transport simulation for the energy range of about 10 eV to 100 GeV. To simulate the ionization processes induced by the charged particles the continuous energy losses model with delta-ray generation including full Vavilov-Landau fluctuations is provided. For calculation of mean or

restricted energy loss for electrons and positrons formulae [27] are used. The density effect and shell correction terms in the stopping power formulas are included. The basic procedure used to calculate the density effect correction is described in [28]. Modified [29] set of the parameters is used. Recently, ICRU-recommended data for collision stopping power of charged leptons in composite materials was included. Multiple scattering of the charged particles is simulated in modified Moliere approximation. Particle path correction due to multiple Coulomb scattering is included in the calculations as well. The discrete bremsstrahlung photon energy is sampled from a Seltzer and Berger [30] differential cross section for electron kinetic energy below 10 GeV and Bethe-Heitler cross section above this threshold. The angular distribution of emitted photon is sampled according to approximation of double differential cross section. A differences between the radiative stopping power for positrons and electrons is included. At very high energies the Landau-Pomeranchuk-Migdal effect is taken into account too.

## 3. BENCHMARK PROBLEM

The benchmark problem was formulated as follows [31]. The target (Fig. 3) consisted of a 7.62 cm – diameter sphere of depleted uranium (0.22 wt % of $U^{235}$) plated with 0.0254 cm of copper and 0.0127 cm of nickel and surrounded by a layer of water $0.20 \pm 0.03$ cm thick and a type 304 stainless steel jacket, 0.07 cm thick. A reentrant hole, 2.54 cm in diameter, admitted the 28 MeV electron beam to within 0.85 cm of the sphere. This hole is also lined with a water jacket.

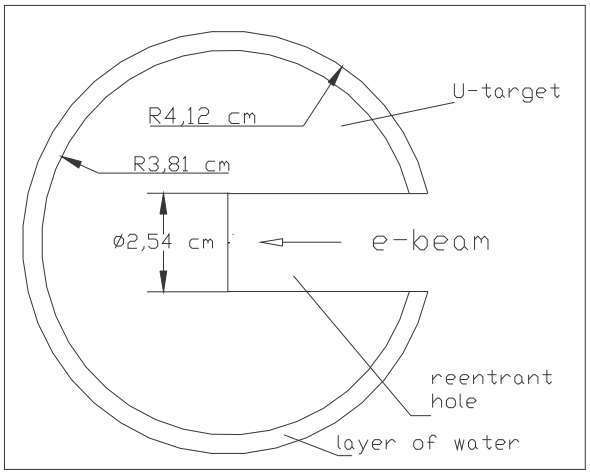


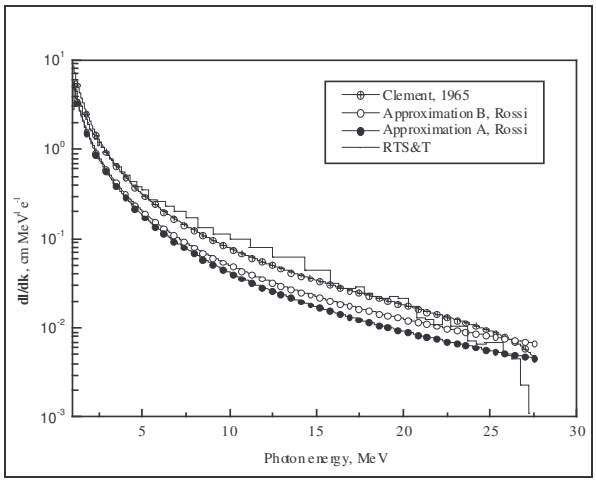


**Figure 3. Schematic target layout.**

**Figure 4. Differential photon track-length distribution produced in uranium target struck by 28 MeV electrons**

Monte Carlo calculations were performed using RTS&T general-purpose code. More details on the code used on can find in the Ref. [32]. Fig. 4 plots the differential track length $dl / dk$

distribution produced in uranium target struck by 28 MeV electrons calculated by RTS&T code in comparison with a three analytical estimating methods are based on Approximations A and B (Rossi , 1952) of electromagnetic shower theory and Clement formula [33], more accurate for photon energies close to that of the primary. Fig. 5 shows the energy distribution of bremsstrahlung photons produced by primary electron inside the target. Fig. 6 displays the hemisphere-integrated leakage spectra, measured by the time-of-flight method compared with RTS&T calculations included a two different photon-nucleus interaction models: data driven model with the BOFOD [34] data files and RTS&T parametrization-driven model in combination with a general data-driven treatment of low-energy nucleon (photon) transport using the ENDF/B-VI data library. The angular distribution of photoneutrons at the target surface is given in Fig. 7 as a cumulative probability vs the cosine of the angle between the radius vector and the direction of the neutron. Numerical data are given by 10 energy groups: 0.200-0.302 , 0.302-0.498, 0.498-0.821, 0.821-1.350, 1.350-2.020, 2.020-3.010, 3.010-4.490, 4.490-6.700, 6.700-10.000, 10.000-15.000 MeV.

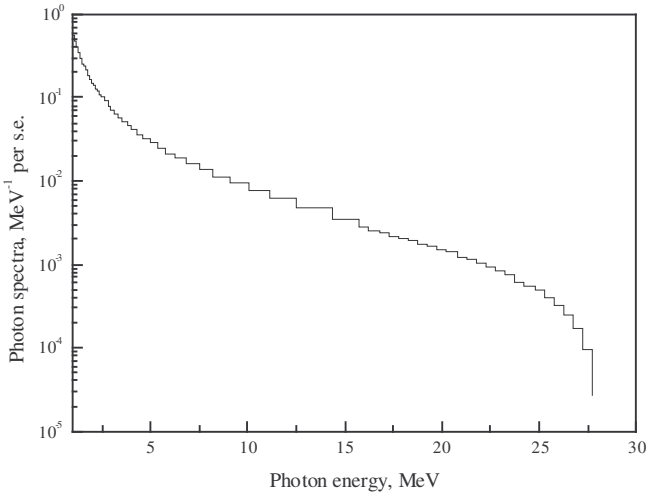


**Figure 5. Bremsstrahlung spectra induced by 28 MeV electrons in uranium target.**

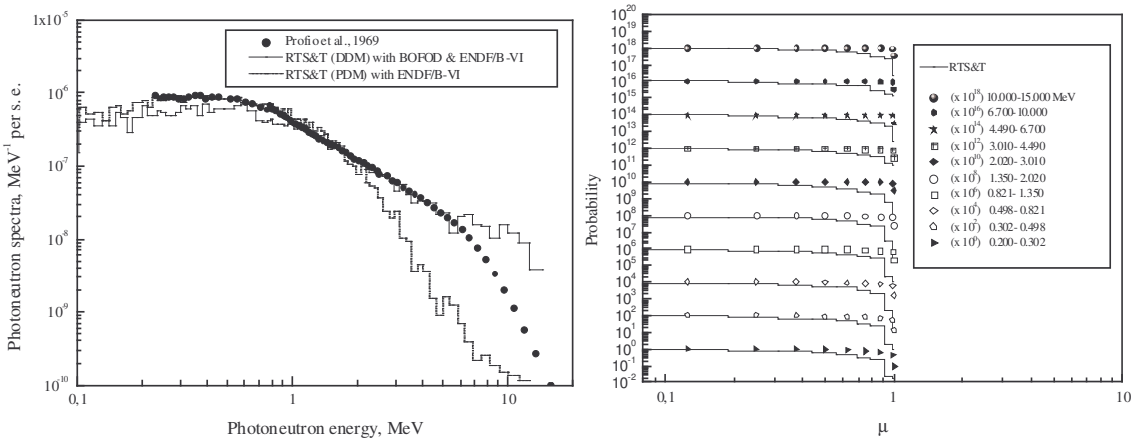


**Figure 6. Comparisons of experimental photoneutron leakage spectrum with calculations using RTS&T code.**

**Figure 7. Cumulative probability for photoneutrons emitted from surface of uranium target.**

## REFERENCES


2. A.I. Blokhin, I.I. Degtyarev, A.E. Lokhovitskii, M.A. Maslov and I.A. Yazynin, *Proceedings of the SARE-3 Workshop*, KEK, Tsukuba, Japan, May 1997.
3. J.D. Jackson, *Canad. J. Phys.* 34 p.767 (1956).
4. W. Dilg et al., *Nucl. Phys.* A217 p.269 (1973).
5. *Reference Input Parameter Library (Handbook for calculations of nuclear reaction data)*, IAEA-TECDOC-Draft, Vienna, March 1998.
6. *Handbook on Photonuclear Data for Applications (cross sections and spectra)*, IAEA-TECDOC-Draft No. 3, Vienna, March 2000.
7. N. Bianchi et al., *Phys. Lett.* B299 p.219 (1993).
8. J. Ahrens et al., *Phys. Lett.* B98 p.423 (1981); B146 p.303 (1984).
9. U. Knessl, *Proc. of Second Intern. Conf. on Dynamical Aspects of Nuclear Fission*, Dubna 1994, p. 28.
10. Th. Frommhold et al., *Phys. Lett.* B295 p.28 (1992).
11. V. Muccifora et al., *LANL arXiv*: nucl-ex/9810015 23 Oct. 1998.
12. P.P. Delsanto, A. Fubini, F. Mirgia and P. Quarati, *Z. Phys*. A342 pp.291-298 (1992).
13. V. di Napoli, *J. Phys.* G15 (1989) L97.
14. M.B. Chadwick and P. Oblozinsky, *Phys. Rev.* C 50 p.2490 (1994).
15. B.S. Sychev, *Cross Sections of High-Energy Hadron Interactions with Atomic Nuclei, Radiotechnical Institute of the USSR Academy of Sciences*, Moscow, 1999.
16. A.S. Iljinov et al., *Nucl. Phys.* A 616 pp.575-605 (1997).
17. *Landolt-Bornstein* , Vol. 8 (New Series), Springer-Verlag (1973).

18. P. Corvisiero et al., *Nucl. Instr. Meth.* A 346 pp.433-440 (1994).
19. V.S. Barashenkov and V.D.Toneev, *Interactions high-energy particles and nuclei with nuclei*, Atomizdat (1972).
20. J.D.T. Arruda-Neto et al., *Nucl. Phys.* A 638 pp.701-713 (1998).
21. A. Lepretre et al., *Nucl. Phys.* A 390 p.221 (1082).
22. M. Effenberger et al., *LANL arXiv*:nucl-th/9607005, 1996.
23. H.C. Fesefeldt, *Technical Report PITHA 85-02*,III Physikalisches Institut, RWTH Aachen Physikzentrum, 5100 Aachen, Germany, Sept. 1985.
24. T. Valentine, *Report ORNL,* TM-1999/300.
25. D.E. Cullen, *IAEA-NDS-39*, Rev. 9 (1996).
26. J. Ranft, *Siegen Univ. Preprints* SI-99-5, SI-99-6, Siegen, Germany.
27. D.E. Cullen et al., *UCRL-50* Vol. 6, 1989.
28. S.M. Seltzer and M.J. Berger, *NASA Publ*. SP-3012.
29. R. M. Sternheimer et al., *At. Data Nucl. Data Tables* 30 p.261 (1984).
30. H. Hirayama, *KEK Internal Report* 95-17.
31. S.M. Seltzer and M.J. Berger, *Nucl. Instr. Meth*. B12 pp.95-134 (1985).
32. A.E. Profio, H.M. Antunez, and D.L. Huffman, *Nuclear Science and Engineering*, 35 pp.91-103 (1969).
33. I.I. Degtyarev, A.I. Blokhin et al., INDC(CCP)-426 pp. 161-188.G. Clement, C.R. Acad. Sci., 257 p.2971 (1963); Thesis 3e Cycle Univ. of Paris, 1964; 28. G. Clement et al., Nuovo Cimento 37 p.876 (1965).
34. A.I. Blokhin et al., BOFOD-99: Present Status of the Evaluated Photonuclear Data File, INDC(CCP)-426, p. 119.